Available online at www.sciencedirect.com
ScienceDirect
Journal of Solid State Chemistry 179 (2006) 3839–3848
JOURNAL OF SOLID STATE CHEMISTRY
www.elsevier.com/locate/jssc

High-pressure growth of $NaMn_7O_{12}$ crystals

Edi Gilioli[a,*], Gianluca Calestani[b], Francesca Licci[a], Carlo Paorici[c], Andrea Gauzzi[d], Fulvio Bolzoni[a], Andrea Prodi[e]

[a]*IMEM—CNR, Area delle Scienze 37/A, 43010 Fontanini—Parma, Italy*
[b]*Dipartimento di Chimica, Università degli Studi di Parma, Area delle Scienze, 43100 Parma, Italy*
[c]*Dipartimento di Fisica, Università degli Studi di Parma, Area delle Scienze, 43100 Parma, Italy*
[d]*Université de Paris VI, Pierre et Marie Curie, 140, rue de Lourmel, 75015 Paris, France*
[e]*MIT, Massachusetts Institute of Technology, 77 Massachusetts Avenue, Cambridge, MA 02139-4307, USA*

Received 2 May 2006; received in revised form 14 July 2006; accepted 16 July 2006
Available online 29 July 2006

Abstract

With the aim of producing large crystals of metastable $NaMn_7O_{12}$ manganite, suitable for physical measurements (i.e.: RXS, Raman, EPR, STS, single-crystal neutron diffraction), we carried out a systematic investigation of the parameters controlling the growth of crystals, including the thermodynamic variables (T, P, and reagent composition) and the kinetic factors, such as reaction time and heating/cooling rate. By varying each parameter while maintaining constant the other ones, we found the thermodynamic conditions under which an optimum equilibrium is reached between the competing nucleation and growth rates. They were found to range between 400 and 700 °C (T) and between 20 and 60 Kbars (P), respectively. Under these conditions, we further optimized the growth process, by establishing the most appropriate growth duration (several hours), reagent type (pre-reacted precursor) and composition (presence of 0.4 mole% water and of 5% Na excess with respect to the stoichiometric composition). Typical crystals having several hundreds μm in linear sizes were reproducibly obtained, while the largest sample was about 800 μm.

A description of the crystal growth mechanism, based on the experimental results, is also presented and discussed. It assumes that two different mechanisms control the crystal growth, depending on whether the crystallization is taking place outside the stability field, i.e. in presence of native reagents, or inside it, i.e. in a polycrystalline $NaMn_7O_{12}$ phase matrix. In the first case, large crystal growth occurs thanks to the low nucleation and high diffusion rates, while in the second one the crystallization is due to the solid-state mechanism based on the free energy reduction caused by grain boundary migration.

Keywords: Single crystal; High pressure; Manganite; $NaMn_7O_{12}$

1. Introduction

$NaMn_7O_{12}$ (hereafter $NaMn_7O_{12}$) is a manganite with a complex perovskite-like structure [1,2]. It is a metastable phase at ambient pressure and only forms under high-pressure conditions. Due to the absence of the chemical disorder which typically occurs in the mixed valence manganites, $NaMn_7O_{12}$ represents a model system for the study of Mn charge, orbital and spin ordering, which can simply be derived from crystallographic data [1]. Due to such peculiarities, it obviously represents a quite interesting system for physical investigations and complex mechanism understanding. The first report on the synthesis of this material was already published in 1973 [2], but only recently it has received a renewed interest, because good quality bulk (polycrystalline) material became available. We already described the synthesis [3], the P/T phase diagram [4] and the growth and the structural refinement of tens micron-sized $NaMn_7O_{12}$ crystals [5]. To clarify the ordering mechanisms, the properties associated with the CE-type magnetic structure and the peculiar orbital occupation in comparison with the classical half-doped manganites [1], large-sized crystals have to be analysed, by, for instance, resonant X-ray scattering (RXS) [6], electron paramagnetic resonance (EPR [7], Raman scattering [8],

*Corresponding author. Fax: +39 0521 269206.
E-mail address: edi@imem.cnr.it (E. Gilioli).

0022-4596/$ - see front matter © 2006 Elsevier Inc. All rights reserved.
doi:10.1016/j.jssc.2006.07.036

scanning tunnelling spectroscopy (STS) [9] and single-crystal neutron diffraction [10].

On the other hand, this system poses a great challenge to the crystal grower. The difficulty in controlling the pressure, as an additional thermodynamic variable, makes severe limitations to the availability of suitable apparatus and the checking of reproducible results.

In this paper, we describe the results of a systematic investigation of several crystal growth parameters and report the optimized conditions for obtaining hundreds μm-size $NaMn_7O_{12}$ crystals. We also present and discuss the crystallization mechanisms, which account for the experimental results and are consistent with the available literature.

2. Apparatus and experimental

2.1. High-pressure apparatus

The $NaMn_7O_{12}$ synthesis and crystal growth take place under high-pressure–high-temperature (HP/HT) conditions. The relevant experiments were carried out in a 6/8-type multi-anvil apparatus using Pt capsules (volume = 58 or 153 mm^3, depending on the assembly type). The capsules (30-μm-thick Pt foil) were inserted in an octahedral MgO assembly and then in the multi-anvil apparatus, in contact with a Pt/Pt—Rh 10% thermocouple for monitoring the temperature during the reaction. The pressure was first increased up to the maximum value at the rate of 160 bar/min. The capsule was then heated up to the maximum temperature at rates varying between 2 and 60 °C/min, kept for 1–4 h and cooled down to room temperature by either switching off the heater, or by applying a controlled cooling rate. Finally, the pressure was released at ≈50 bar/min. In some experiments, the assembly was mounted with two or three capsules, each one filled with a different precursor. In such a "multi-capsule system" two or more reactions take place under identical conditions, thus avoiding uncontrolled variations of pressure or temperature.

Calibration experiments carried out on standard materials show that the temperature and pressure gradients inside the capsule are negligible.

2.2. Solid-state synthesis and crystal growth

Stoichiometric and 5–10 mol% Na-rich mixtures of Mn-oxides (MnO_2 Alfa Aesar, 99.9% and Mn_2O_3 Ventron, 98%) and NaOH pellets (Merck, >99%) were used as reagents. Alternatively, a pre-reacted precursor was used. It was obtained by mixing stoichiometric (or Na-rich) amounts of Mn- and Na-citrate solutions. The mixed solution was gelled by slowly evaporating and the solid residual heated at 750 °C for 24 h. More details on the procedure are reported in [11]. The precursor looks like a fine black powder, whose main components are Mn_2O_3 and $Na_2Mn_5O_{10}$. No oxidizing/reducing agents were ever used to modify the reaction atmosphere.

The reagents/precursors were mixed, finely grounded in a glove box to prevent hydration, and encapsulated in the Pt foil (not sealed).

Once the capsule is removed from the multi-anvil apparatus, the reaction products are easily recovered, by cutting the capsule with a blade.

2.3. Characterization

Powder X-ray diffraction (XRD) were performed on a X-ray Siemens D-500 diffractometer with a Cu$K\alpha$ ($\lambda = 1.540$ Å) radiation. From the powder diffraction we determined the sample composition and semi-quantitatively evaluated the content of different phases by refining the data with the GSAS programme and by using the available structural model [12].

A Philips PW1100 single-crystal diffractometer equipped with graphite-monocromatized Mo$K\alpha$ ($\lambda = 0.71069$ Å) radiation was used for the crystal structure determination and refinements. The data were collected at room temperature on single crystals mechanically separated from the powders.

Simultaneous differential scanning calorimetry (DSC) and thermogravimetry (TG) were made in a Netzsch 409/429 apparatus, under normal atmosphere and in alumina crucibles.

The crystals were isolated and measured by optically observing under a Leica DC300 F microscopy.

SEM images were taken by a Cambridge Stereoscan 360 scanning electron microscope (SEM).

3. Results and discussion

The solid-state synthesis of $NaMn_7O_{12}$ carried out under the conditions delimiting the P/T stability region [2], yields polycrystalline, μm-size powders, 99% single-phase. Typical products obtained at 700 °C and 60 Kbar, after 2 h-reaction, are shown in Fig. 1. By reacting a non-stoichiometric precursor containing 100% [Na] excess for 10 h at $P = 60$ Kbar and $T = 830$ °C and by cooling down to 600 °C at a rate of 10 °C/h, $NaMn_7O_{12}$ crystals with average linear dimensions of 20–40 μm were obtained. A SEM picture of the best crystals grown under such conditions is shown in Fig. 1(b). From the solid matrix, a 75-μm crystal (linear dimensions) was mechanically separated and used for single-crystal X-ray structure determination [4].

With the aim of increasing the crystal size, we tried different approaches, by taking into account several significant parameters. We firstly tried to optimize the kinetics of crystallization by moving inside the stability field of the $NaMn_7O_{12}$ phase (Fig. 2, left side). We either increased the reaction time (up to 160 h) and decreased the heating/cooling rate (±2 °C/h). We also introduced small crystals within the reagents in order to provide seeds for preferential crystallization and crystal growth. Then, we

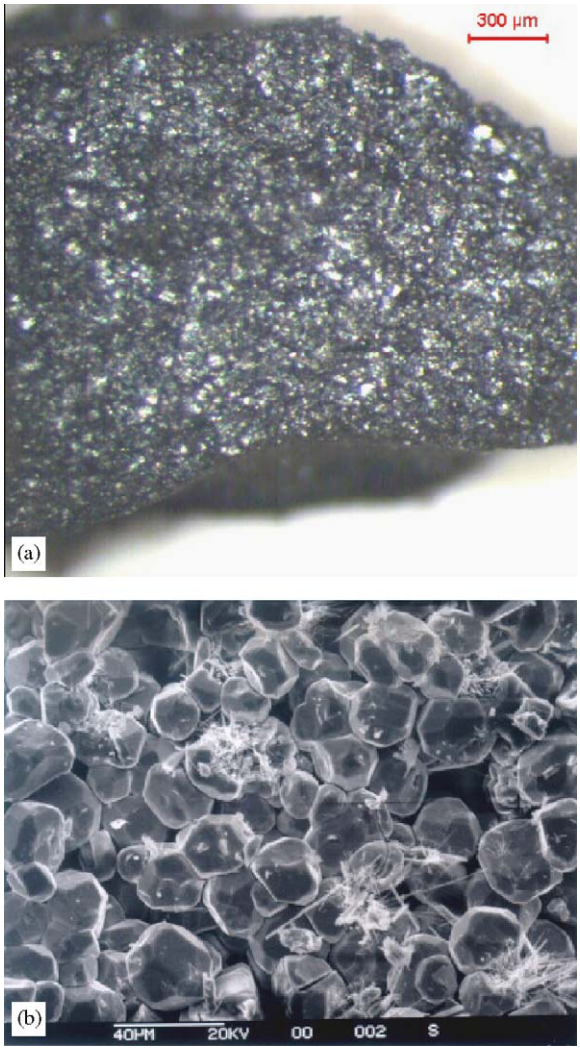

Fig. 1. Optical (a) and SEM images (b) of $NaMn_7O_{12}$ crystals. Note the markers: 300 μm, top-right corner (a) and 40 μm, bottom left (b).

varied the reagent composition by adding small amounts of water, to simulate a hydrothermal synthesis, or by increasing the Na content (up to 300% with respect to the stoichiometric amount), to promote the formation of some "flux". None of these attempts gave any significant improvement. Finally, we explored the P/T space outside the thermodynamic stability field. In the upper side, we increased T up to 1100 °C and P up to 60 Kbar, trying to induce the melting and melt-growth processes. On the opposite side, we reduced T and P down to values belonging to the lower left portion of the phase diagram (red square in Fig. 2). Under these "mild" conditions we finally succeeded in enlarging the crystal sizes and we could define the appropriate P/T conditions (Fig. 2, right panel) for growing larger crystals.

In order to compare the reaction products and to point out the dependence of the crystal growth results on the reaction conditions, we used optical and electron microscopy observation and X-ray powder and single-crystal diffraction, whenever the crystals were present, sampled in different regions of the capsule. The average size among different experiments was assumed to be similar within 15% difference. The crystals were easy to be optically detected, due to their shining silvery aspect, well distinguishable from the embedding grey powders. The results are presented in a pictorial way; all the optical images presented hereafter (and Fig. 1(a), as well), have the same marker (300 μm, top-right corner), to make the comparison easier among different experiments.

3.1. Effect of temperature and pressure

In Figs. 3 and 4 we show the effects of temperature and pressure on the crystal growth, by referring to the phase diagram of Fig. 2, right side. The effect of temperature

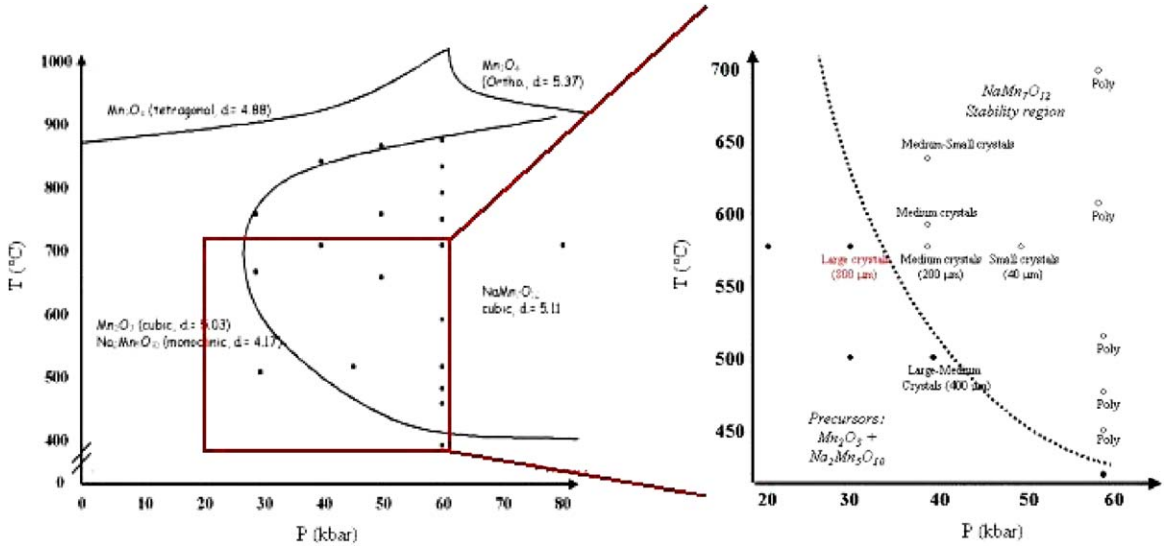

Fig. 2. Enlarged area of $NaMn_7O_{12}$ phase diagram. Left diagram is taken from [3].

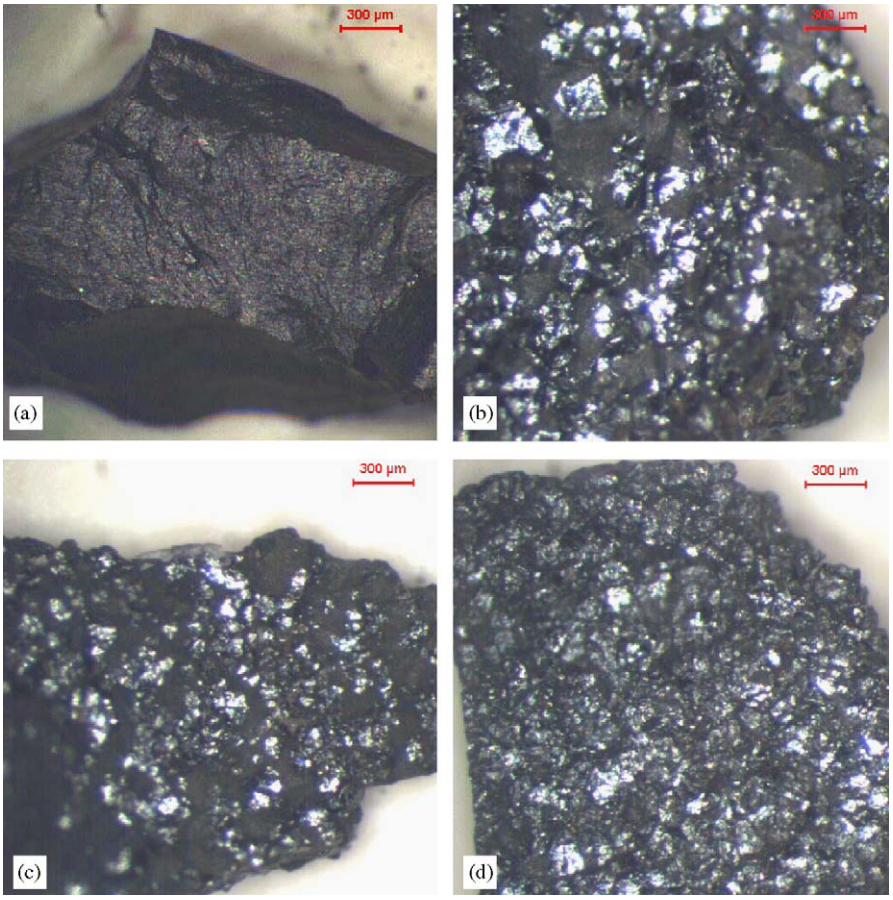

Fig. 3. Effect of T on $NaMn_7O_{12}$ crystal size: (a) $T = 400\,^{\circ}C$, (b) $500\,^{\circ}C$, (c) $575\,^{\circ}C$ and (d) $650\,^{\circ}C$. $P = 40$ Kbar, reaction time = 2 h, reagents = precursor with 5% [Na] excess.

(Fig. 3(a)–(d)) was determined by varying T and keeping constant the other parameters: ($P = 40$ Kbar, reaction time = 2 h, reagents = 5% Na excess precursor). Analogously, the effect of pressure (Fig. 4(a)–(d)) was determined by varying P under constant T (= 575 °C), reaction time (= 2 h), and reagent type (= 5% Na excess precursors).

The results can be described as in the following:

(a) At T and P lower than those defining the $NaMn_7O_{12}$ stability field (Fig. 2), no crystals are present (Figs. 3(a) and 4(a)) and the X-ray patterns indicate the presence of the Mn_2O_3 and $Na_2Mn_5O_{10}$ reagents.
(b) Crystals form and grow when moving towards the precursors/$NaMn_7O_{12}$ transition curve. They reach the largest dimensions at the external border of the curve (Figs. 3(b) and 4(b)). After mechanically separating the crystals, XRD of the matrix in this region still show the presence of starting reagents.
(c) By further increasing T and P, i.e. entering the $NaMn_7O_{12}$ stability field, the crystals remain present but smaller (Figs. 3(c) and 4(c)). XRD of the polycrystalline matrix shows the presence of the $NaMn_7O_{12}$ phase in addition to the reagents (mainly Mn_2O_3).
(d) Finally, (Figs. 3(d) and 4(d)) the crystals get smaller and smaller when moving into the high P/T region. The optical images in these case are similar to that of polycrystals (Fig. 1(a)) and XRD indicate that products are almost 100% $NaMn_7O_{12}$.

On the basis of these experiments we conclude that:

(a) The P/T phase diagram of the $NaMn_7O_{12}$ phase we proposed in [3] is consistent with the new experiments.
(b) "Large" $NaMn_7O_{12}$ crystals are obtained in the narrow portion of the P/T phase diagram, across the transition curve. The better results (3–400 μm average crystal size) are obtained under the conditions of Figs. 3(b) and 4(b), outside (but close to) the thermodynamic stability field. Crystals are embedded in the reagent powders. The largest specimen (800 μm, Fig. 4(b)) grew from a 5% [Na] excess precursor, after a 2-h reaction at $T = 575\,^{\circ}C$ and $P = 30$ Kbar.
(c) When moving within the thermodynamically optimized crystal growth field, the crystallization process can further be improved, by systematically adjusting the process variables.

In the following, we report the effects due to several significant parameters.

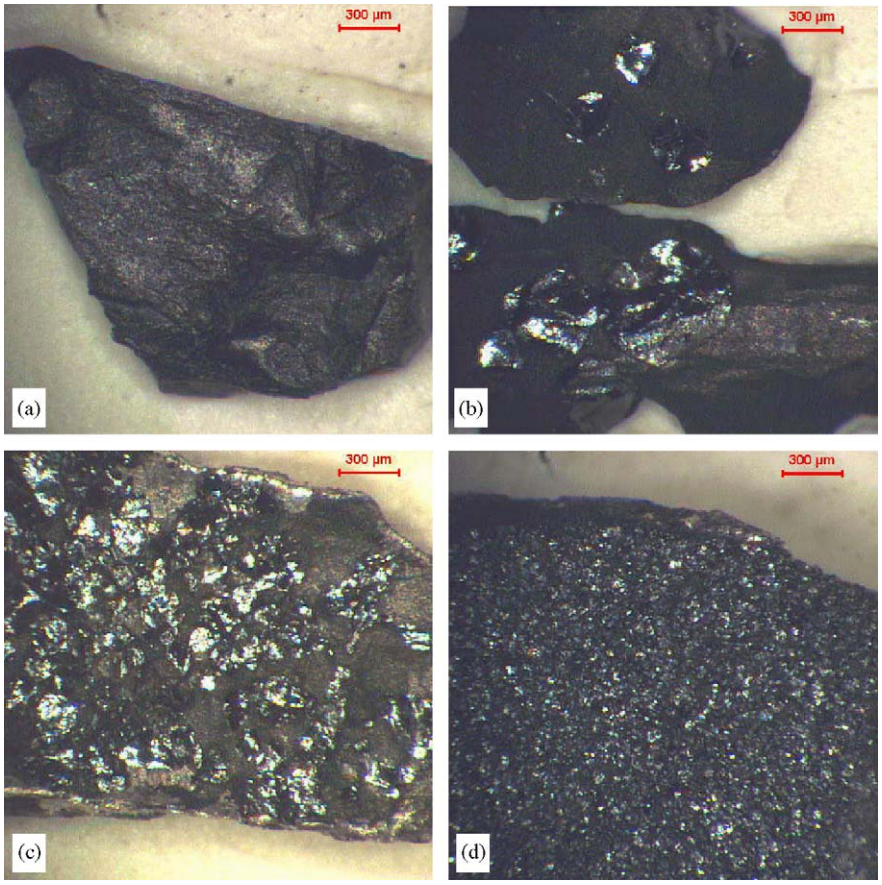

Fig. 4. Effect of P on $NaMn_7O_{12}$ crystal size: (a) $P = 20$ Kbar, (b) 30 Kbar, (c) 40 Kbar and (d) 50 Kbar. $T = 575\,^{\circ}C$, reaction time = 2 h, reagents = precursor with 5% [Na] excess.

3.1.1. Reaction time

The reaction time was one of the parameters that appeared to have no influence on the crystal size in the experiments carried out under high P/T conditions. It indeed may play a significant role, when working in the appropriate thermodynamic field. $NaMn_7O_{12}$ crystals obtained at $P = 30$ Kbar, $T = 575\,^{\circ}C$, are presented in Fig. 5 after 10 min (Fig. 5(a)), 2 h (Fig. 5(c)) and 31 h reaction (Fig. 5(e)), together with the collection of isolated single crystals (Fig. 5(b), (d), and (f), respectively).

Surprisingly, 100–180-μm-sized, facetted crystals were observed already after few minutes reaction (Fig. 5(a)–(b)). The crystals in Fig. 5(d) are among the best we obtained from the structural point of view; they exhibit a complex polyhedral shape. Longer reaction time induces the merging of adjacent crystals, leading to bigger masses of crystalline agglomerates, that usually break when trying to separate them from the powdered matrix (Fig. 5(f)).

3.1.2. Heating/cooling rate

The heating or cooling rate does not affect the crystal growth of $NaMn_7O_{12}$, either in the high P/T region and in the optimized crystal growth field.

By varying the heating rate from 2 to 60 °C/min, we do not appreciate any significant difference in the average size of crystals. We conclude that the effective parameter is the total reaction time, regardless of the heating velocity.

3.1.3. H_2O content

We noticed that the $NaMn_7O_{12}$ crystallization was somehow dependent on the aging of the precursor, the crystal size resulting larger when aged precursors were used. In several cases no crystals at all could be obtained from freshly prepared precursors. DSC/TG thermal analysis proved that the precursors, although kept in a dry atmosphere, tends to hydrate, as a consequence of the hygroscopic properties of the Na–Mn–O compounds. The DSC plots of fresh and aged precursors are compared in Fig. 6. The DSC peak at about 100 °C clearly indicates that the aged material releases some humidity. The process is reversible and a 1-h annealing at 150 °C is sufficient to recover the dry reagents. TG analysis indicates that the absorbed water is about 0.4% (w/w) of the total mass, which corresponds to a $NaMn_7O_{12}/H_2O$ molar ratio ≈ 8.

In Fig. 7(a) and (b), we compare $NaMn_7O_{12}$ samples, obtained in a double-capsule experiment, from a dry and a hydrated precursor, respectively. The other process variables were: $P = 30$ Kbar, $T = 575\,^{\circ}C$, time = 2 h, reagent = 5% [Na] excess precursor. The precursor was annealed 1 h at 150 °C, to get a dry compound, and then

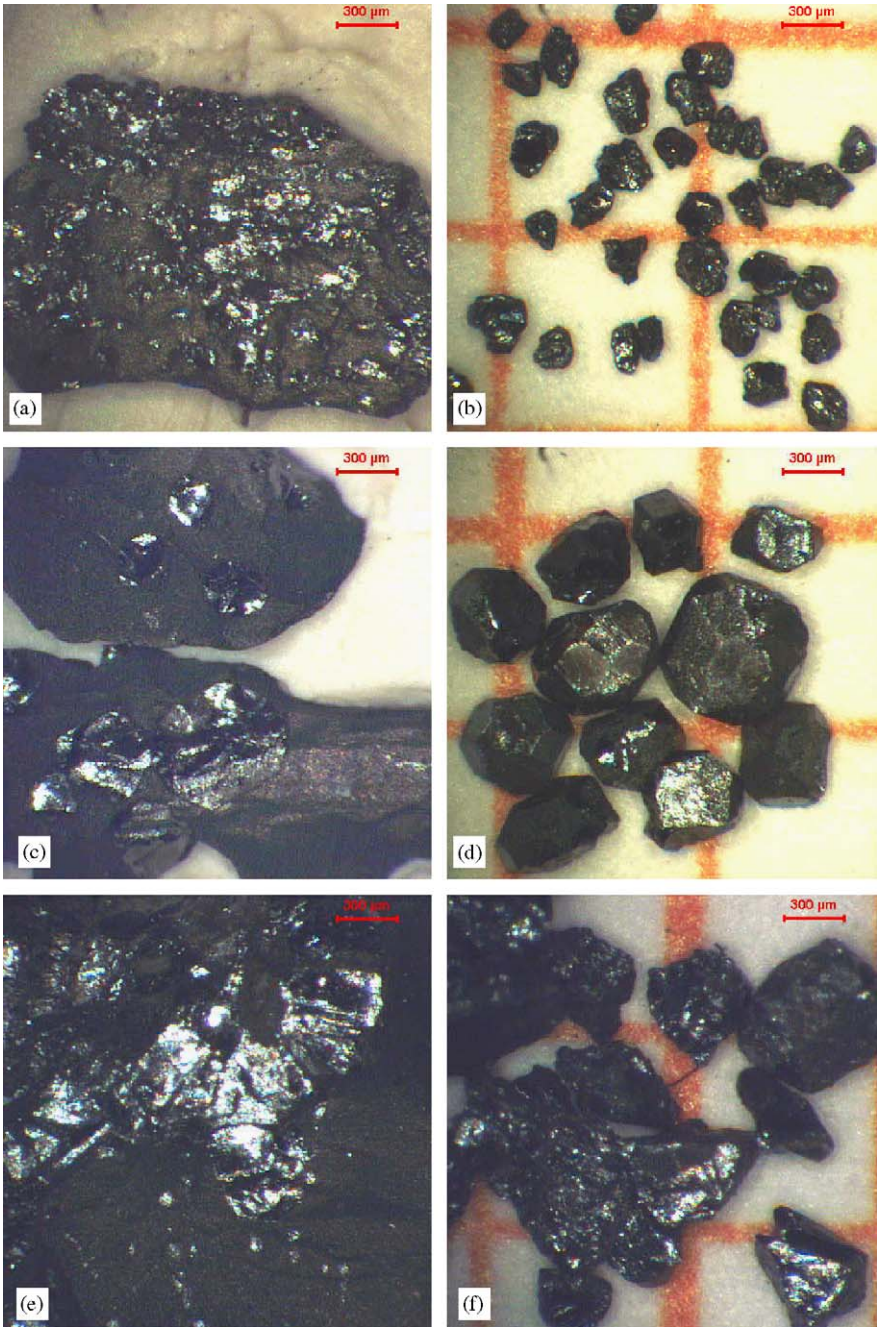

Fig. 5. Effect of reaction time on $NaMn_7O_{12}$ crystal size. (a, b) 10 min, (c, d) 2 h and (e, f) 31 h. $T = 575\,^{\circ}C$, $P = 30$ Kbar, reagents = precursor with 5% [Na] excess.

it was divided in two portions. In one case, it was used as it was (dry precursor), in the second one it was added with 0.6 μL distilled water (hydrated precursor, with a $NaMn_7O_{12}/H_2O$ molar ratio ≈ 8). The pictures clearly demonstrate that the presence of H_2O favors the crystallization of $NaMn_7O_{12}$. On the other hand, the crystal sizes did not improve with an increase in the water amount. Both these results were reproduced several times, by repeating the experiments under similar conditions.

3.1.4. *Na excess*

The effect of the Na content in the precursors has been extensively studied, since it significantly affects the $NaMn_7O_{12}$ phase quality and the crystal growth.

In the case of the $NaMn_7O_{12}$ synthesis, we demonstrated that the optimal Na content in the precursors is a 5% excess with respect to the stoichiometric ratio [3,4]. At lower Na concentration, a significant amount of Mn_2O_3 remains in the products, while traces of secondary phases appear in the XRD patterns if the Na excess is increased up

to 10% or more. Although the spurious phases could not be precisely identified, their weight fraction increases with increasing the Na concentration and therefore can be tentatively attributed to Na-rich Na–Mn-oxides.

As far as the crystal growth is concerned, we found that a small excess of Na improves the nucleation and crystal growth. Fig. 8 shows crystals obtained from dehydrated precursors, varying Na excesses ($T = 575\,^{\circ}C$, $P = 30$ Kbar and reaction time = 2 h, were kept constant). One notices that no crystals form for Na content up to 5% excess (Fig. 8(a)); large crystalline conglomerates appear when [Na] excess is 10% (Fig. 8(b)), whereas they become smaller and more dispersed by increasing Na excess to 15% (Fig. 8(c)). This finding suggests that Na favors the nucleation process. We hypothesize that the presence of Na and H_2O in the regents are related, Na–Mn–O compounds being hygroscopic, and that both of them play a role in the crystallization process. A reasonable connection between the two variables could be that the higher the Na content, the easier (or faster) the hydration which allows the minimum amount of water to trigger the crystal growth. However, we point out that the results described in Fig. 8 only refer to the Na presence, because, as confirmed by TG checking, any absorbed water was removed by dehydrating the precursors at 150 °C for 90 min. The full understanding of Na and water interplay deserves further investigations, which are presently in progress.

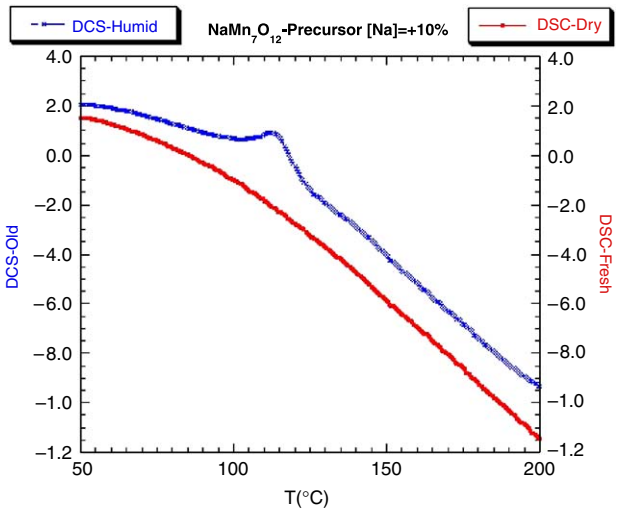

Fig. 6. DSC plot of "fresh" (red line) and "aged" (blue) precursor.

3.1.5. Reagent type

The reacting mixture was considered as an additional process variable, by comparing the $NaMn_7O_{12}$ crystallization yield when using as reagents either commercial oxides or sol–gel precursors.

In order to properly compare the effect of the reagents, the corresponding high-pressure crystal growth experiments were carried out in parallel, under identical conditions, by using the double-capsule system.

Typical results are shown in Fig. 9(a) and (b). They demonstrate that much larger crystals are obtained when sol–gel precursors are used. The experiment was repeated several times, giving reproducible results in about 80% of the cases, thus confirming that finer and better-dispersed powders yield faster kinetics and improved products.

In a few cases, however, we were not able to grow $NaMn_7O_{12}$ crystals in spite of applying the optimized procedure. In all these cases, we could associate the lack of crystallization to the occurrence of "anomalous" XRD patterns of the precursor. The black, extremely fine precursor powders, from which $NaMn_7O_{12}$ crystallizes, are a mixture of Mn_2O_3 and $Na_2Mn_5O_{10}$, (ICDD card no 27-0749). On the contrary, the "anomalous" precursors which seem to inhibit the crystallization were found to consist of $Mn_2O_3 + Na_4Mn_9O_{18}$ (ICDD card no 27-0750). Since identical sol–gel process were used in all the experiments, we are at the moment unable to explain the difference, but we intend to further investigate the subject in order to achieve a better control of the reaction and a correct understanding of the role of different Na–Mn oxides in the crystallization.

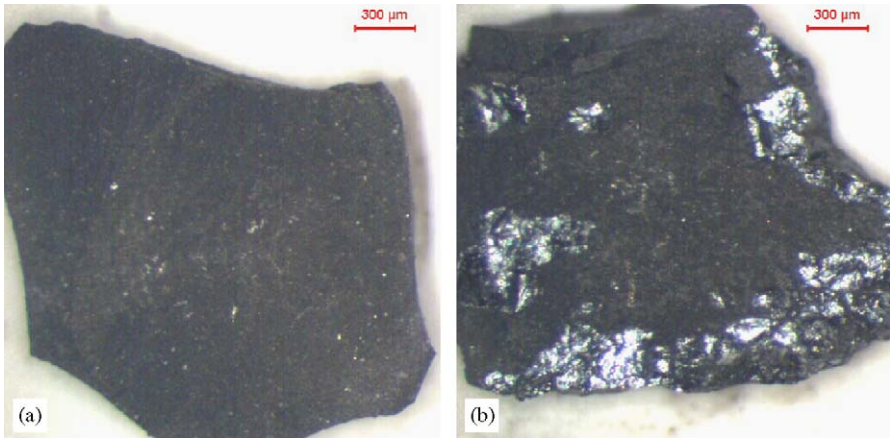

Fig. 7. Effect of H_2O on $NaMn_7O_{12}$ crystal size, Dry (a) and hydrated precursor (b) are compared. $T = 575\,^{\circ}C$, $P = 30$ Kbar, reaction time = 2 h, reagents = precursor with 5% Na excess.

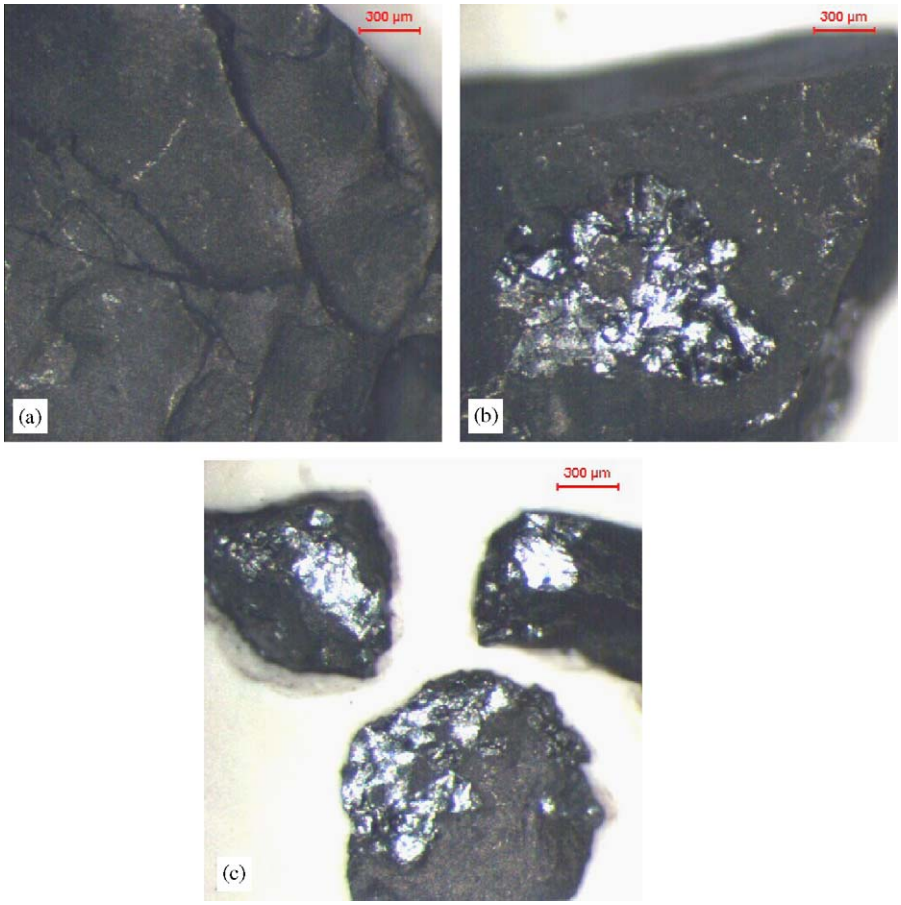

Fig. 8. Effect of [Na] excess on $NaMn_7O_{12}$ crystallization when starting from a dehydrated precursor. Na stoichiometric excess is 5% (a), 10% (b), 15% (c), respectively. ($T = 575\,^{\circ}C$, $P = 30$ Kbar, reaction time = 2 h).

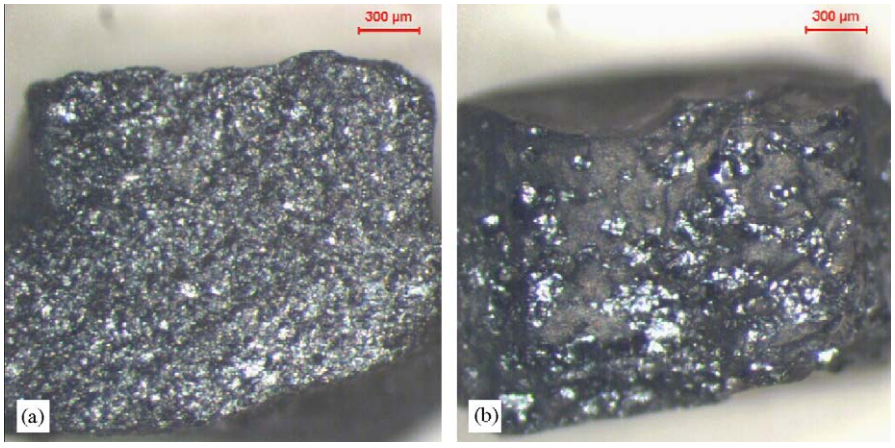

Fig. 9. Effect of the use of oxide and precursor on $NaMn_7O_{12}$ crystal size. Reagents were oxides in (a), and precursors in (b). The experiments were done in the same run, with the double-capsule assembly. The other parameters were $T = 575\,^{\circ}C$, $P = 40$ Kbar, reaction time = 2 h.

3.2. Crystallization mechanism

Due to the high-pressure and the relatively low-temperature conditions, it seems unrealistic to hypothesize the presence of significant quantities of liquid phases during the crystallization process. Consistently, no traces of a liquid solidification are detectable in the reaction capsule after the experiments, thus supporting the assumption that $NaMn_7O_{12}$ prevalently crystallizes in a solid-state environment. On the other hand, it has to be pointed out that the largest crystals grow in a "mild" thermodynamic regime, under moderate pressure and temperature conditions and they are embedded in the reagent precursors, i.e. outside the macroscopic stability field of the $NaMn_7O_{12}$

phase. Under such conditions, quite large crystals form in relatively short time (Fig. 5). On the contrary, smaller crystals segregate from the $NaMn_7O_{12}$ matrix inside the compound stability field, and they get smaller and smaller when increasing temperature or pressure (Figs. 3 and 4). Under such a regime, even the increase of the growth time seems to be detrimental for the crystal quality and morphology, in contrast with the well-established fact that the efficiency of the secondary crystallization increases by increasing the reaction duration, temperature and pressure. We suggest that the anomalous behaviour we observe may be explained by assuming two different mechanisms driving the crystallization, in presence of the precursors (outside the stability field) or of $NaMn_7O_{12}$ phase (inside the stability field).

In the precursor crystallization case, the $NaMn_7O_{12}$ nucleation takes place at the thermodynamically appropriate T and P conditions, but the relevant rate remains quite low due to the mild regime. On the contrary, once the nucleus critical sizes have been reached, the growth kinetics is relatively high, as a consequence of the presence of traces of water (expected to be supercritical under the experimental conditions, Fig. 7) and of the very reactive, atomically dispersed precursor grains (Fig. 9). Both factors keep the average ion diffusion to the growing crystal surface higher than solid-state diffusion in water-free and mechanically dispersed reagents. The combined effects of the low nucleation rate and the high diffusion kinetics yield few and large crystals in relatively short time. The crystals result well separated from the embedding friable precursors.

When T and/or P are increased, entering the $NaMn_7O_{12}$ stability region, the nucleation rate increases much more than the growth rate and the two processes compete. The nucleation involves the whole sample and the precursor quickly transforms into fine-grained polycrystalline $NaMn_7O_{12}$. In such a regime we hypothesize that the crystal growth mechanism is a solid-state one.

In spite of the extensive literature covering the solid-phase re-crystallization of metals [13], when moving to non-metallic materials, as in the case of magnetic compounds, the available references appear to be much more restricted, especially when the grain growth process occurs under elevated pressures. It is, however, generally accepted that, also in the case of ceramic compounds, the solid-phase re-crystallization leading to the growth of one (or a few) grain is the result of grain-boundary migrations similar to those observed in metals. The minimization of the surface energy would ultimately made the boundaries migrate away from the larger grains, leading to a final state in which the polycrystalline structure is transformed into few lattice regions. A first experimental evidence dates back to more than 50 years ago [14]. Accordingly, the growth of crystals from polycrystalline $NaMn_7O_{12}$ could be explained as a high-pressure–high-temperature process in which the crystal undergoes a free energy reduction by migration (and size reduction) of grain boundaries. These boundaries are indeed zones of higher free energy in a polycrystalline structure when compared to a single-crystal one. In a first stage, the $NaMn_7O_{12}$ particles coalesce in a porous fine-grained matrix and subsequently sinter. The vacancies, by which the pores are made up, diffuse to the boundaries, thus causing the pores to shrink. Such pore shrinking would be favoured [15–18] by high vacancy diffusivity as well as by elevated pressures. The evidence that traces of water improve the crystallization while larger quantities do not can be accounted for by considering that large water inclusions in the pores would hinder their shrinking, and limit the sintering process. According to the theory [16,17], sintering by pore shrinking is also favoured by fine grain size, with respect to larger and non-homogeneous particles. The sintering process finally leads to the formation of a polycrystalline structure practically free from pores and made up of a reduced number of grains with different size, differently oriented with respect to each other and separated by transition zones (grain boundaries). The final state, in which the polycrystalline structure is transformed into one or few lattice regions with the same orientation can now be achieved when the grain boundary movement reduces the free energy. A quantitative treatment of the process is presently out of reach, but, qualitatively, it can be surmised that the boundary movement (and that of vacancies in a counter-stream), would take place when, upon heating, the atomic vibrations increase enough that movements of atom become possible. However, as was observed experimentally, at too high temperatures, the efficiency of the crystallization process appears to be reduced (Fig. 3). This is probably related to the fact that the pore shrinking stage turns out to be limited when the temperature increases too much [15].

4. Conclusions

We succeeded in reproducibly obtaining crystals of $NaMn_7O_{12}$ as large as several hundred μm in linear dimensions, necessary for physical experiments aimed to study the ordering (charge, orbital and spin) phenomena present in this material.

The largest crystal we separated was about 800 μm large. Such a crystal grew under moderate T and P conditions, around the border which separates the instability from the stability field in the P/T $NaMn_7O_{12}$ phase diagram.

The systematic optimization of the kinetic factors, such as growth duration and heating/cooling rate, as well as the use of pre-reacted precursors containing small amounts of water and Na excess, allowed improving the crystal size and morphology.

To account for the experimental findings, we propose that two different mechanisms control the crystal growth, depending on whether the process is taking place outside the $NaMn_7O_{12}$ stability field, i.e. in presence of the native precursor) or inside it (i.e. in a polycrystalline $NaMn_7O_{12}$ matrix). In the first case, we assume that large crystals segregate as a consequence of the competing low nucleation

rate and high diffusion rate, the latter being favored by the presence of supercritical water and fine-grained reagents. The second crystallization process is suggested to be a solid-state one, driven by sintering. The crystals in this case grow in the solid phase as a consequence of the larger grain boundary migration toward the smaller ones, and the associate release of the free energy.

Acknowledgments

The authors acknowledge M. Marezio for stimulating the research interest, T. Besagni for X-ray and DTA/TG analysis, P. Ferro for precursors preparation, C. Orecchia for optical images and G. Salviati for SEM analysis.

References

[1] A. Prodi, E. Gilioli, A. Gauzzi, F. Licci, M. Marezio, F. Bolzoni, Q. Huang, A. Santoro, J.W. Lynn, Nat. Mater. 3 (2004) 48–52.
[2] M. Marezio, P.D. Dernier, J. Chenavas, J.C. Joubert, J. Solid State Chem. 6 (1973) 16–20.
[3] E. Gilioli, G. Calestani, F. Licci, A. Gauzzi, F. Bolzoni, A. Prodi, M. Marezio, Solid State Sci. 7 (2005) 746–752.
[4] E. Gilioli, G. Calestani, F. Licci, A. Gauzzi, F. Bolzoni, A. Prodi, M. Marezio, J. Cryst. Growth 275 (2005) e877–e880.
[5] E. Gilioli, F. Licci, G. Calestani, A. Prodi, A. Gauzzi, G. Salviati, Cryst. Res. Technol. 40 (10/11) (2005) 1072–1075.
[6] Y. Mrakami, J.P. Hill, D. Gibbs, M. Blme, I. Kayoma, M. Tanaka, H. Kawata, T. Arima, Y. Tokra, K. Irota, Y. Endoh, Phys. Rev. Lett. 81 (1998) 582.
[7] R. Gupta, J.P. Joshi, S.V. Bhat, A.K. Sood, C.N.R. Rao, J. Phys: Condens. Matter 12 (2000) 6919–6926.
[8] S. Yoon, M. Rübhausen, S.L. Cooper, K.H. Kim, S.-W. Cheong, Phys. Rev. Lett. 85 (2000) 3297–3300.
[9] Ch. Renner, G. Aeppli, H.M. Ronnow, Mater. Sci. Eng. C25 (2005) 775–778.
[10] A. Daoud-Aladine, J. Rodriguez-Carvajal, L. Pinsard-Gaudard, M.T. Fernandez-Diaz, A. Revcolevschi, Phys. Rev. Lett. 89 (2002) 097205.
[11] F. Licci, G. Turilli, P. Ferro, A. Ciccarone, J. Am. Ceram. Soc. 86 (2003) 413.
[12] A.C. Larson, R.B. Von Dreele, General structure analysis system (GSAS), Los Alamos National Laboratory Report LAUR 86-748, 2000.
[13] J.C. Brice, Crystal Growth Processes, Wiley, New York, 1986 (Chapter 11).
[14] M.J. Buerger, E. Washken, Am. Miner. 32 (1947) 296.
[15] G.M. Fryer, Trans. Br. Ceram. Soc. 66 (1967) 127.
[16] F.A. Kröger, The Chemistry of Imperfect Crystals, North-Holland, Amsterdam, 1964 (Chapter 21).
[17] M.B. Waldron, B.L. Daniell, Sintering, Heyden and Son Powder Technology Series Publications, 1978.
[18] Sintering Processes, in: C.G. Kuczynski (Ed.), vol. 13, Plenum press, New York, 1980.